JAAS

Accepted Manuscript

This is an *Accepted Manuscript*, which has been through the Royal Society of Chemistry peer review process and has been accepted for publication.

Accepted Manuscripts are published online shortly after acceptance, before technical editing, formatting and proof reading. Using this free service, authors can make their results available to the community, in citable form, before we publish the edited article. We will replace this *Accepted Manuscript* with the edited and formatted *Advance Article* as soon as it is available.

You can find more information about *Accepted Manuscripts* in the Information for Authors.

Please note that technical editing may introduce minor changes to the text and/or graphics, which may alter content. The journal's standard Terms & Conditions and the Ethical guidelines still apply. In no event shall the Royal Society of Chemistry be held responsible for any errors or omissions in this *Accepted Manuscript* or any consequences arising from the use of any information it contains.

ROYAL SOCIETY OF CHEMISTRY

www.rsc.org/jaas

Laser Produced Plasma Diagnosis of Carcinogenic Heavy Metals in Gallstones

Mohammad A. Gondal[a*], Mohamed A. Shemis[a], Ahmed A. I. Khalil[b,c], Mohamed M. Nasr[d], Bilal Gondal[e]

[a]Physics Department, King Fahd University of Petroleum & Minerals, Dhahran 31261, Saudi Arabia

[b]Physics Department, Faculty of Science for Girls, University of Dammam, Dammam 31113, Saudi Arabia

[c]Department of Laser Sciences and Interactions, National Institute of Laser Enhanced Sciences, (NILES), Cairo University, Giza 12613, Egypt

[d]Preparatory Health Department, Riyadh Colleges of Dentistry and Pharmacy, Riyadh 11343, Saudi Arabia

[e]Department of Gastroenterology, The University of Chicago Pritzker School of Medicine, Chicago, IL 60637, USA

*Author for correspondence:

Prof. M.A. Gondal, Department of Physics, King Fahd University of Petroleum &Minerals,

Box 5047, Dhahran-31261, Saudi Arabia.

Fax: +966138602293; Telephone: +966138602351

E-mail: magondal@kfupm.edu.sa

Abstract

Gall bladder cancer [GBC] is a highly fatal malignancy. Geographically regions of high prevalence of gallstones [GS] have shown to have higher rates of GBC, which is now a recognized risk factor for GBC. Heavy metals toxicity has also been reported to associate with GBC. An effort therefore at recognizing and avoiding potential risk factors for GBC occurrence is therefore paramount. It is also known that over the time heavy metals can accumulate in the biliary system and hence in the GS. We hereby measured the levels of heavy metals in GS via a highly sensitive technique using laser produced plasma comparing levels of heavy metals in a 29 years old man to a 65 years old man. For this direct spectral analysis of GS, laser produced plasma was created by focusing 266 nm pulsed UV laser generated by fourth harmonics of Nd:YAG laser on GS samples. For the first time to the best of our knowledge, the plasma parameters, electron temperature and electron density for GS matrix were computed from the Boltzmann distribution of the upper energy levels and Stark broadening of selected spectral lines. The plasma parameters determination is important to satisfy the optically thin plasma (to avoid self-absorption) and obtain local thermodynamic equilibrium (LTE) conditions, which are critical for the quantitative analysis. The heavy metal concentrations of chromium, lead, cadmium, nickel and mercury were determined in two different GS samples by recording the laser induced breakdown spectra (LIBS) and by drawing the calibration curves of the spectral lines of carcinogenic metals like chromium, lead, cadmium, nickel and mercury. The results obtained from LIBS were crosschecked using a standard inductively coupled plasma-mass spectrometer (ICP-MS) technique. The effect of delay time (time between the laser pulse and the ICCD camera gate opening) and laser energy on the intensity of the spectral lines of lead, chromium and calcium were also investigated. The system developed in this study is highly applicable for rapid analysis of any biological or human tissue samples.

Keywords: Medical Optics Instrumentation, Laser Induced Breakdown Spectroscopy, toxic metals detection, gallbladder stones.

Introduction

The key role of gallbladder [GB] is storing bile that is produced by the liver to be released in the duodenum during digestion [1]. The incidence of GS disease is on the rise. According to the third National Health and Nutrition Examination Survey 6.3 million men and 14.2 million women aged 20 to 74 in the United States had GB disease [2]. GS fall into two categories: cholesterol and pigment stones, which mainly consist of cholesterol, calcium salts and bilirubin [3]. Environmental pollution and smoking can increase the level of toxic metals like chromium [Cr], lead [Pb], nickel [Ni], cadmium [Cd] and chromium [Cr] in the body over time [4-6]. It has been stated previously that contamination of drinking water with toxic metals such as Cr, Pb and Cd increases their level in the human body, which leads to higher levels in the biliary system and GS [7]. Rise of heavy metals toxicity is also associated with the GBC and other organs [7, 8]. The constituents of GS can be Ca, Na, Cl, K, Mg, Mn, Fe, P, Cu, Pb, Ti, Zn, Al, Ni and Cr. This has been found previously using expensive techniques like X-ray fluorescence or neutron activation analysis technique [9, 10].

We applied laser induced breakdown spectroscopy (LIBS) technique, which is based on inducing high temperature (more than 5000 K) plasma using highly energetic (~ 40 mJ) laser pulses. The constituting elements can be identified from their finger-print spectral lines, and their concentrations can be calculated from the spectral lines intensities similar to many of the other spectroscopy-based analytical techniques. LIBS is a fast, portable, in-situ and remote analyzing technique, and capable of detecting and determining concentrations of few ppms with little or no sample preparation. For in-situ and low limit of detection analysis, LIBS spectrometer can be built by using a pulsed laser source, a spectrometer, fast electronics, an intensified charge coupled device (ICCD) camera and a computing device.

In this work, the concentrations of toxic elements Cr, Pb, Ni, Hg and Cd were determined in two different samples of GS obtained surgically from a young 28 years and an older 65 years old man, using LIBS technique. The observed spectral lines wavelengths were matched with the finger-print spectral lines of the elements available from the spectral lines database published by national institute of standards and technology (NIST) [11]. By applying LIBS technique to standard samples of known concentrations, we could plot the intensities of the spectral lines versus element concentrations which are known as calibration curves. The toxic metals concentrations in the two GS samples were then determined by measuring their spectral lines intensity and thus calculating the corresponding concentrations on the calibration curves. The toxic metals concentrations in the GS were also measured by inductively coupled plasma-mass spectrometer (ICP-MS) technique to validate our results obtained by LIBS technique. Plasma temperature and electron density were estimated from the Boltzmann distribution of the upper energy levels and the spectral lines broadening of the strongest calcium lines respectively, to assure that optically thin plasma and local thermal equilibrium prevails. Optically thin or non-self-absorbing plasma condition is critical for elements detection, calibration and accurate concentration measurement [10, 12-18].

Experimental Methods

LIBS Principle

In our experiment, high temperature (~ 17000 K) plasma was induced on the sample surface using extremely powerful laser pulses having about 40mJ pulse energy and 8ns pulse width. The evolution of laser induced plasma goes through several stages in the first few microseconds after laser ignition. In the first stage, material surface heating, evaporation, and then thermionic emission and molecule dissociation take place. Second, plasma ignition, atomic excitation and

ionization, and atomic and ionic emission take place. Finally, plasma expansion and cooling take place [10]. The induced plasma spectrum is then analyzed with a high resolution spectrometer. The identification of the induced spectral lines is carried out using spectral lines database to find the corresponding elements from their finger-print wavelengths.

Experimental Setup

We utilized an Nd:YAG laser with a wavelength of 266 nm, a pulse width of 8 ns, a frequency of 20 Hz and an energy in the range of 12.5 and 35 mJ for GS sample ablation. Laser was directed toward the sample surface and focused with a quartz convex lens of 50 mm focal length, while the sample was rotated using a rotary table in order to prevent crater formation and shifting the focal point on the sample surface. The induced spectrum was recorded in the region of 270-850 nm, which has most of the neutral and singly ionized atomic spectral lines, using a high resolution (0.1 nm) spectrometer (Andor SR 500 i-A) that has a grating with 600 line/cm groove density and an optical fiber at an angle of 45^{o}. The ICCD camera (Andor- iStar) was synchronized with the laser pulses in order to control the delay time which is the time between the laser ignition and ICCD camera gate opening, and the gate pulse width which is the spectrum recording time after each laser pulse. Singh and co-workers [19] applied a pulsed Nd:YAG laser with a wavelength of 532 nm, a pulse duration of 3 – 4 ns (FWHM), a frequency of 10 Hz and very high energy of 425 mJ for GS sample ablation. They focused the laser at the surface of the stone by utilizing a quartz lens of short focal length = 15 cm and used multichannel grating spectrometer (Ocean Optics, LIBS 2000+ software) which is not sensitive and of high resolution as compared with our time resolved gated ICCD (Andor SR 500 i-A) spectrometer. In our system one can use different delay times and could resolve spectrum at time scale 0.1 nsec. In this experiment, the delay time was in the range 25-500 ns, and the gate width was 40 μs. The

accumulation number and number of scans were optimized to be 20. Many other parameters in the LIBS system can affect the induced plasma properties, spectral lines intensities and thus the accuracy of LIBS system such as the main components in target sample, geometrical setup of the lenses, mirrors, sample and optical fiber at ambient conditions (atmospheric pressure and temperature). Before recording the LIBS spectrum, the two gallstones were polished, cleaned with ethanol and set at the focal point of the convex lens. Fig. 1 shows a photograph of the typical gallstone sample placed on a tap to prevent the displacement due to the high power laser.

The procedure for the ICP-MS analysis and sample preparation is briefly explained below.

For ICP-MS, 0.01 g of a GS sample was added into 5 ml of nitric acid (HNO3) with 99 % purity (Fisher Scientific), the solution was heated at 60 ^{0}C until the nitric acid reduces to 2 ml, to ensure complete dissolution in the acid solution. The solution is allowed to cool, after which 40 ml of water was added and further heated at 45 ^{0}C for 2 hours to allow complete digestion of the GS sample. The resulting solution after cooling was sieved into to a volumetric flask to remove any undissolved particles and then deionized, double distilled water was then added to get 50 ml solution. The resultant solution was then analyzed using ICP-MS after thorough mixing. These steps were repeated for the each sample.

Approval was obtained from "Alhada Military Hospital Al-Taif Saudi Arabia" for the analysis of gallstones from the involved patients for this case study. Both patients were also notified of the purpose of the research study and gave informed consent for their gallstones to be used for this particular research. Ethics committee approval was also obtained from the registrar [approval dated 24-11-2015] for collection of gallstones samples at the urology department Alhada Military Hospital Al-Taif Saudi Arabia. In addition, all procedures performed in this study involving human participants were in accordance with the ethical standards of King Fahd

University of Petroleum &Minerals and with the 1964 Helsinki declaration and its later amendments or comparable ethical standards.

Results and discussion

Spectrum (Qualitative and Quantitative) Analysis

The laser induced spectra of the two GS samples were recorded in the region 270-850 nm under the conditions of 400 ns delay time, 40 mJ laser energy and 266 nm laser wavelength. Most of the observed spectral lines and their corresponding elements were identified, as shown in Figs. 2 and 3. The identification of the atomic transition lines was carried out using the spectral lines database provided by NIST [11]. The existence of the constituting elements was confirmed by identifying three finger-print spectral lines of each element or more. The constituting elements are divided into two categories, major elements (Ca, Na, Mg, K, Fe, Zn, Cl and Cu) and toxic elements (Cd, Ni, Cr, Pb and Hg). Table 1 summarizes the concentrations of the toxic elements and the spectral assignments of the observed spectral lines which were used in calculating plasma temperature and electron density. We presented the qualitative and quantitative results on measurement of carcinogenic elements like Cd, Cr. Pb, Hg and other metals like Zn and Ni present in Gall bladder stone samples which were also confirmed by ICP-MS analysis in our case so our data is more authentic in that sense while Singh and co-workers [19] detected by LIBS technique in the center and shell parts only Ca, Mg, Mn, Cu, Fe, Na, K, Sr, Zn, C, H, N, O, and P and were not able to detect the carcinogenic elements like Cd, Cr, Pb and Hg due to low sensitivity of their LIBS system. All experiments were carried out in atmospheric pressure in air. This is the reason for the presence of a marginal fraction of oxygen line in the spectrum.

Optically thin plasma and local thermodynamic equilibrium (LTE) condition were satisfied due to high electron density and Maxwellian distribution of the velocity. Optically thin plasma is required to have the accurate LIBS analysis. Optically thin plasma guarantees that there is no self-absorption of the emission lines in the plasma. For optically thin plasma and local thermodynamic equilibrium condition, the spectral line intensity can be written as follows:

$$I_{ik,z} = \frac{A_{ik,z} g_{i,z} L \cdot N_z}{\lambda_{ik,z} U_z(T)} \exp\left(-\frac{E_{i,z}}{KT}\right), \quad (1)$$

where $I_{ik,z}$ is the relative intensity due to electron transition from a high state i to a lower state k in an atom with ionization z, $E_{i,z}$ corresponds to the upper energy level and $g_{i,z}$ is its statistical weight, $A_{ik,z}$ is the transitional probability, $\lambda_{ik,z}$ is the spectral line wavelength, $U_z(T)$ is the atomic partition function at temperature T, L is the plasma characteristic length, N_z is the emitting atoms density, K is the Boltzmann constant and T is the plasma temperature [18, 19].

Standard samples of previously known concentrations were used to draw calibration curves of the spectral line intensity versus element concentration for the lines Cd I 291.5, Pb I 368.3, Cr I 425.4, Ni I 361.9 and Hg I 366.3, as shown in Fig. 4. Furthermore, these elements concentration in the two gallstones were determined from the laser plasma induced spectral lines intensity by locating the line intensity on the calibration curve, as listed in Table 1. In addition, elements concentrations were measured using inductively coupled plasma mass spectroscopy (ICP-MS) technique as explained earlier under experimental section to validate our LIBS results, as listed in Table 1. Results presented in Table 1 show that the level of toxic elements [Pb, Cd, Cr, Hg] are higher in the 65 years old person compared to the 29 years old person.

Delay Time and Laser Energy Effects

Figure 5 depicts the intensities of the spectral lines Pb I 363.3 and Ca II 393.4 at different delay times. The figure 5 shows that the spectral line intensity decreases with the increase in the delay time. It is clear that the dominant contribution in the spectral lines intensities occurs in the first 500 ns. We studied the temporal distribution of plasma parameters T_e and N_e of GS, while, Singh et. al. [19] have studied the spatial distribution of Cu and Mg in black pigment of GS. We studied the temporal distribution only and spatial distribution will be investigated in the future work. Thus the spatial non-uniformity of laser-induced plasmas is not considered. In addition, we investigated the average temperature and electron density for the plasma for all elements where the temperature is almost the same for different elements in GS under same laser fluence. The measurement of electron temperature and electron density is important to make sure that our laser induced plasma is not thick to avoid any self-absorption. In addition, the intensities of the three lines Ca II 396.8, Pb I 368.3 and Cr I 425.4 nm increase linearly as the laser energy increases in the range 12.5-45 mJ, as shown in Fig. 6, while, Singh and co-workers [19] did not study this phenomenon. From the above mentioned comparison, it clearly reveals that our experimental setup and results are different and more accurate than Singh et al [19] results and reflects to our novelty in this work.

Temperature and Electron Density Calculations

In order to satisfy optically thin plasma and LTE conditions, the measurement of electron density is highly desirable. For one atomic species in ionization state *z,* whereas N_z and $U_z(T)$ are constant, the spectral line intensity equation (Eq. 1) reduces to

$$ln\left(\frac{I_{ik,z}\lambda_{ik,z}}{g_{i,z}A_{ik,z}}\right) = -\frac{E_{i,z}}{KT} + \text{constant.} \quad (2)$$

By calculating the left hand side expression and plotting versus $E_{i,z}$ for the spectral lines of some atomic species in the ionization state z, the temperature can be calculated from the slope $1/KT$. The main source of error in calculating T arises from the inaccuracy of ln ($A_{ik,z}$) [16, 20]. Eq. 1 was applied on the strongest observed spectral lines of the singly ionized sodium and calcium ions, Na II lines at 297.7, 316.4, 371.1 and 411.4 nm and Ca II lines at 315.9, 317.9, 393.4 and 396.8 nm as depicted in Fig. 7. The parameters λ, $A_{ik,z}$, $g_{i,z}$ and $E_{i,z}$ were taken from the references [11, 21-23]. The average of the estimated plasma temperature for 266 nm, 40 mJ laser and 400 ns delay time was around 17200 K.

For accurate elemental LIBS analysis, LTE must exist in optically thin plasma. An electron density for LTE condition was calculated using Mcwhirter criteria

$$n_e \geq 1.4 \times 10^{14} T^{\frac{1}{2}} (\Delta E)^3 \mathrm{cm}^{-3} \quad (3)$$

where n_e and ΔE are the electron density and the largest transition energy corresponding to the shortest wavelength used in temperature calculation [16]. Broadening of plasma spectral lines originates from Stark effect (caused by energy levels splitting due to plasma induced electric field and has FWHM ~ 0.1-1 nm), the Doppler effect (caused by the thermal motion of the ions and has FWHM ~ 0.01-0.1 nm), the Van Der Waals effect (caused by Van Der Waals' dipolar force, negligible in high ionized plasma and has FWHM ~ 0.01 nm) and instrumental reasons [24, 25]. The spectral line broadening in plasmas is affected by Doppler, pressure and Stark broadening. In this work, because the plasma produced by the laser reveals low temperatures and densities, the contributions by Doppler, Van der Waals, and resonance broadening are negligible for the Ca II at 393.4 nm which had been used to determine the electron number density. The contribution to the width is almost due to the electron impact and Stark broadening. The Stark width parameter (ω) of this line is 0.0065 [26, 27]. Since the Stark effect

broadening dominates and, thus, is used to estimate the electron density from the full width at half-maximum (FWHM) of the singly ionized calcium line at 393.4 *nm*. Stark broadening is described by Lorentzian function, and the FWHM is directly proportional to the electron density:

$$\Delta\lambda_{FWHM}(A) = 2\omega\left(\frac{n_e(cm^{-3})}{10^{16}}\right) \quad \text{---------- (4)}$$

where ω is the FWHM of Stark broadening at an electron density of 10^{16} cm^{-3} obtained from Griem's book by interpolating at the calculated plasma temperature [28]. The Stark width is extracted by de-convolution of the instrumental width from the observed line width (FWHM) determined by the least squares fits of a Lorentzian function. Two spectroscopic parameters are used in LIBS to compute the electron density. The first method needs measurement of the Stark broadening of spectral lines and the second needs measurements of the population ratio of two successive ionization levels of the same element. The emission spectral lines of the laser produced plasma are broadened; hence electron density (n_e) can be evaluated from the width of the spectral lines. In our LIBS plasma, two main line broadening mechanisms are Stark broadening and Doppler broadening. Stark broadening is induced by collisions of the emitting atoms with charged species dominant at higher plasma densities. In our work, the Doppler width was computed for the Ca transition. The width is very small to be recorded. Ca II has small oscillator strength, thus this part could be cancelled. If the full width at half maximum (FWHM) of the line $\Delta\lambda_{FWHM}$ (nm) is recorded for Ca II line at 393.4 nm whose shape numerically matches with the Lorentzian profile as depicted in Fig. 8. The electron density can be calculated from the FWHM of Ca II line. The registered line shape was fitted correctly by deducting the instrumental width using a de-convolution process, such as the following:

$$\Delta\lambda_{true} = \Delta\lambda_{observed} - \Delta\lambda_{instrument} \quad \text{..... (5)}$$

The corresponding relative error is approximately 10%. We used a narrow line width at λ = 266 nm to measure the instrumental line width of the UV-LIBS system and it was 0.05 nm. Figure 8 shows the data points and the Gaussian fitting of Ca II 393.4 spectral line with a FWHM of 0.75 nm. Thus, the electron density at 266 nm, 40 mJ laser, 400 ns delay time and 17200 K was calculated to be 3×10^{18} cm^{-3} which was one order of magnitude higher than the estimated minimum electron density 5.7×10^{17} cm^{-3}; hence in our experiment the laser induced plasma was optically thin and in LTE. The temperature and electron density calculations are in good agreement with Ref. [29]. In addition, Fig. 9 shows the calculated plasma temperature and electron density at different delay time values. The results showed that plasma temperature and electron density were about 16000 K and 10^{18} cm^{-3} in the first microsecond, however they sharply decreased to about 9000 K and 10^{16} cm^{-3} after laser ignition by about 4 μs, respectively. Our results showed that Mcwhirter criteria was satisfied at a delay time less than 2 μs, A minimum electron density for LTE condition was calculated using Mcwhirter criteria. The temperature was almost the same for different elements that means we are in LTE i.e. thin plasma state while in thick plasma the temperature varies for different elements. Since Mcwhirter criteria is clearly satisfied which indicates that our plasma is thin so there is no chance of any self-absorption and thus the concentration measured with our LIBS instrument are more accurate. In order to verify Our LIBS results, we also cross checked our results using standard method like ICP-MS and our LIBS results are in excellent agreement with ICP-MS results.

Conclusion

Gall Stones (GS) laser induced plasma was generated and studied in detail for the spectral chemical analysis by applying 266 nm pulsed Nd:YAG laser and using a spectrometer equipped

with an ICCD camera for the detection of toxic heavy metals in GS samples. The temporal behavior of plasma parameters like plasma density and plasma temperature were investigated to prove that our laser induced plasma is in local thermodynamic equilibrium and thus there is no self-absorption of atomic emission lines. Laser induced plasma spectra were recorded for qualitative and quantitative analysis of GS. We found that the dominant contribution in the spectral lines intensity occurred in the first 500 ns, and the lines intensities increase linearly with the increase in laser energy. The observed atomic spectral lines and the constituting toxic elements Cr, Pb, Ni, Cd and Hg were identified using the spectroscopic database published by NIST. In addition, the concentrations of these elements were calculated by plotting the calibration curves using standard samples. The results obtained from LIBS system were also verified by recording the ICP-MS spectrum and our results are in excellent agreement with those obtained from ICP-MS technique. Heavy metals can rise in our body as we grow and age. Our results confirm this rise in concentration of toxic heavy elements when we compared levels in GS of an old person to a young person. This study has demonstrated that our highly sensitive system can be applied for the rapid analysis of human tissue and other biocompatible samples, and secondly proposes a basis for further studies on levels of carcinogens and incidence of GBC.

Acknowledgement

This work was supported by University of Dammam under the project # 2014101. Physics Department and King Fahd University of Petroleum and Minerals support are also gratefully acknowledged through project # RG 1421-1. Dr. Ibrahim Salman, a consultant Urologist, and the Medical Laboratories Center in Al-Hada Military Hospital in Taif, are acknowledged for supplying the authors with samples.

References

1. J. M. Diamand, "The Reabsorptive Function of the Gall-Bladder", J. Physiol. 161(3), 442-473 (1962).

2. J. E. Everhart, M. Khare, M. Hill, K. R. Maurer, "Prevalence and ethnic differences in gallbladder disease in the United States", Gastroenterology 117, 632- 639 (1999).

3. A. T. Al-Kinani, D. E. Watt, B. W. East and I. A. Harris, "Minor and trace element analysis of gallstones", Analyst 109(3), 365-368 (1984).

4. M. Bogunia, B. Ahnert, J. Kwapuliński ,B. Brodziak-Dopierała, J. Kowol, E. Nogaj, E. Bogunia and U. Oleśkow, "Chromium in hydroxiapatites of gallstones from active and passive smoking and nonsmoking women", Przegl Lek. 65(10), 524-528 (2008).

5. Shigeta, S. Ratanamaneechat, S. Srisukho, M. Tanaka, Y. Moriyama, S. Suwanagool and M. Miki, "Epidemiological correlation between chromium content in gallstones and cholesterol in blood", J Med Assoc Thai. 85(2), 183-194 (2002).

6. S. Pervez and G.S. Pandey, "Toxic metals status in kidneys and gallstones of workers in a steel plant environment", Environmental Monitoring and Assessment 32(2), 93-99 (1994).

7. V. K. Shukla, A. Prakash, B. D. Tripathi, D. C. S. Reddy and S. Singh. "Biliary heavy metal concentrations in carcinoma of the gall bladder: case-control study", BMJ 317(7168), 1288-1289 (1998).

8. S. Basu, M. K. Singh, T. B. Singh, S. K. Bhartiya, S. P. Singh and V. K. Shukla, "Heavy and trace metals in carcinoma of the gallbladder", World J Surg 37(11), 2641–2646 (2013).

9. O. A. Golovanova, L. V. Bel'skaya and N. Yu. Berezina, "Quantitative spectral trace element analysis of pathogenic biominerals from residents of the omsk region", Journal of Applied Spectroscopy 73(6), 886-891 (2006).

10. M. A. Gondal, M. H. Shwehdi, and A. A. I. Khalil, "Applications of LIBS for determination of ionic species (NaCl) in electrical cables for investigation of electrical breakdown", Applied Physics B: Lasers and Optics, 105(4), 915-922 (2011).

11. Atomic spectra database, National Institute of Standards and Technology (NIST), http://www.nist.gov/physlab/data/asd.cfm

12. A. A. I. Khalil, M. A. Gondal, M. A. Shemis, and I. S. Khan. "Detection of carcinogenic metals in kidney stones using ultraviolet laser-induced breakdown spectroscopy", Applied Optics 54(8), 2123-2131 (2015).

13. M. A. Gondal, T. Hussain, Z. H. Yamani, and M. A. Baig, "Detection of heavy metals in Arabian crude oil residue using laser induced breakdown spectroscopy", Talanta 72(5), 642–649 (2007).

14. M. A.Gondal, M. M.Nasr, M. M. Ahmed, Z. H. Yamani and M. S. Alsalhi, "Detection of lead in paint samples synthesized locally using-laser-induced breakdown spectroscopy", Journal of Environmental Science and Health Part A 46(1), 1–8 (2011).

15. Y. W. Maganda, Development of A laser Induced Breakdown Spectrometer for Detection of Toxic Elements in Cosmetic Products, Master Thesis. KFUPM, KSA (2000).

16. M.A. Gondal, Y. W. Maganda, M. A. Dastageer, F. F. Al Adel, A. A. Naqvi and T. F. Qahtan, "Detection of carcinogenic chromium in synthetic hair dyes using laser induced breakdown spectroscopy", Applied Optics 53(8), 1636-1643 (2014).

17. A. A. I. Khalil, M.A. Gondal, M. A. Dastageer, "Detection of trace elements in nondegradable oragnic spent clay waste using optimized dual-pulsed laser induced breakdown spectrometer", Applied Optics 53(8), 1709-1717 (2014).

18. M. A. Gondal, M. A. Dastageer, A. A. Naqvi, A. A. Isab and Y. W. Maganda, "Detection of toxic metals (lead and chromium) in talcum powder using laser induced breakdown spectroscopy", Applied Optics 51(30), 7395-7401 (2012).

19 Vivek K. Singh, Vinita Singh, Awadhesh K. Rai, Surya N. Thakur, Pradeep K. Rai, and Jagdish P. Singh, Quantitative analysis of gallstones using laser-induced breakdown spectroscopy, Applied Optic 47(31), G38-G47 (2008).

20. A. Alonso-Medina, "Experimental determination of the Stark widths of Pb I spectral lines in a laser-induced plasma", Spectrochimia Acta Part B: Atomic Spectroscopy 63(5), 598–602 (2008).

21. J. E. Sansonettia, "Wavelengths, Transition Probabilities, and Energy Levels for the Spectra of Sodium (Na I–Na XI)", J. Phys. Chem. Ref. Data, 37(4), 1659-1763 (2008).

22. D. E. Kellehera and L. I. Podobedovab, "Atomic Transition Probabilities of Sodium and Magnesium. A Critical Compilation", J. Phys. Chem. Ref. Data 37(1), 267-706 (2008).

23. P. L. Smith, C. Heise, J. R. Esmond and R. L. Kurucz, "Atomic spectral line database from CD-ROM 23 of R. L. Kurucz." (1995), http://www.cfa.harvard.edu/amp/ampdata/kurucz23/sekur.html

24. J. Torres, J. M. Palomares, Sola A, J. van der Mullen and A. Gamero, "A Stark broadening method to determine simultaneously the electron temperature and density in high-pressure microwave plasmas", J. Phys. D: Appl. Phys. 40(19), 5929 (2007).

25. Z. Qiuping, C. Cheng and M. Yuedong, "Electron Density and Temperature Measurement by Stark broadening in a Cold Argon Arc-Plasma Jet at Atmospheric Pressure", Plasma Science and Technology 11(5), 560-563 (2009).

26. N. Konjevic and W. L. Wiese, Experimental Stark widths and shifts for non-hydrogenic spectral lines of ionized atoms, J. of Physical and Chemical Reference Data, 5, 259 (1976), doi: 10.1063/1.555533

27- H. –J. Kunze, Introduction to Plasma Spectroscopy (Springer Series on Atomic, Optical, and Plasma Physics Press. Heidelberg, 2009)].

28. H. R. Griem, Spectral Line Broadening by Plasmas, McGraw-Hill, New York, 1974.

29. C. Aragón, J. A. Aguilera and J. Manrique, "Measurement of Stark broadening parameters of Fe II and Ni II spectral lines by laser induced breakdown spectroscopy using fused glass samples", J. of Quant. Spect. & Rad. Tran. 134, 39-45 (2014).

Fig. 1. Gallstone sample was placed on a gluey substance to avoid the displacement of GS test samples under the high power laser fluence.

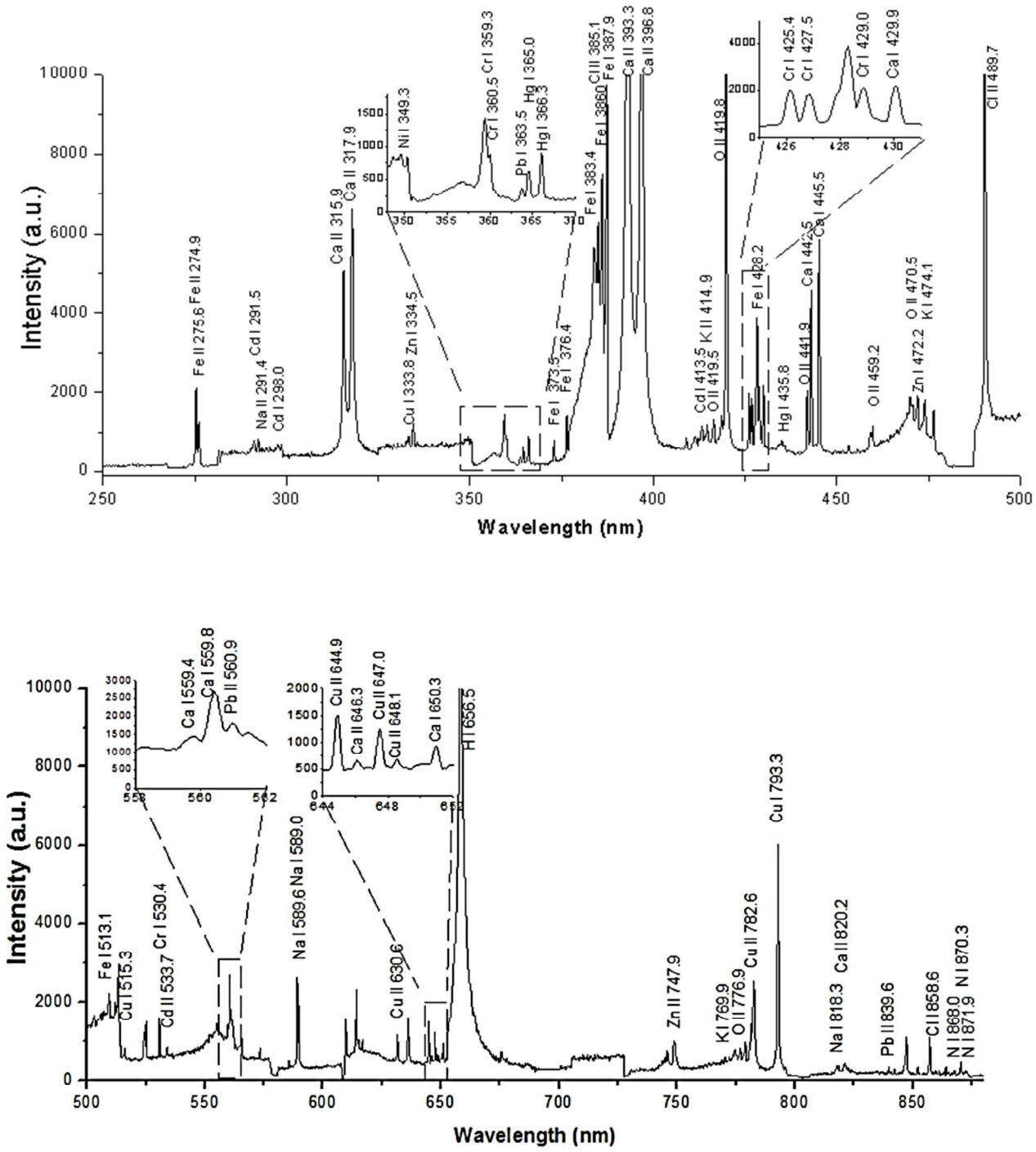

Fig. 2. LIBS spectrum of the first gallstone sample recorded at delay time of 400 ns, laser pulse energy 40 mJ and wavelength of 266 nm.

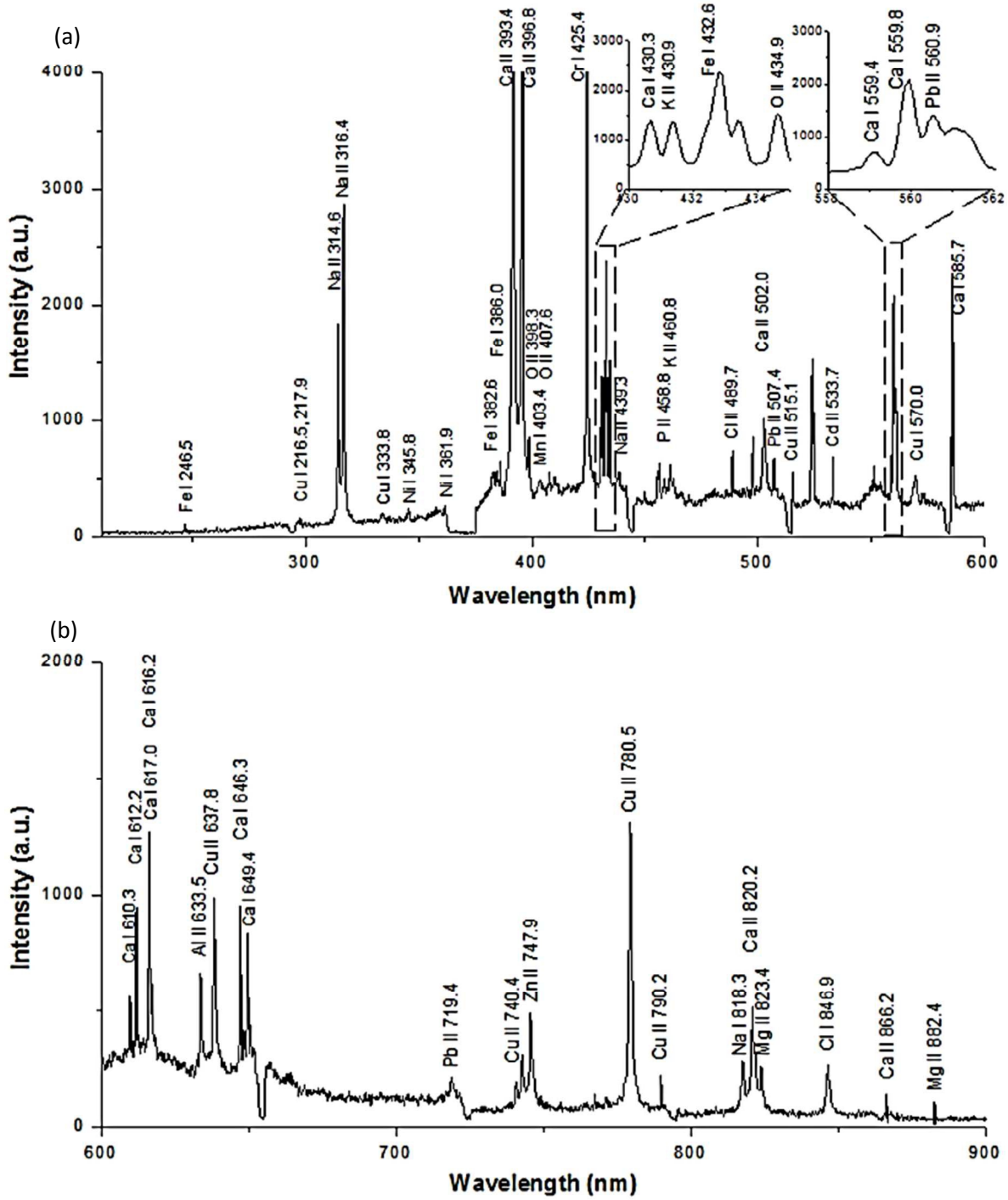

Fig. 3(a,b). LIBS spectrum of the second gallstone sample recorded at a delay time of 400 ns, laser pulse energy of 40 mJ and wavelength of 266 nm.

Table 1: Toxic elements detected, their finger print wavelengths and concentrations in the two GS samples investigated in this study.

Element and ionization degree	Lines Wavelengths (nm)	Concentration (ppm) GS # 1		GS # 2		Spectroscopic notation of transition	Transitional probability (10^8 s^{-1})
		LIBS	ICP	LIBS	ICP		
Cr I	425.4 427.5	.6205	.6517	.451	.528	$^7p_4$-$^7s_3$ $^7p_3$-$^7s_3$	1.5 1.62
Hg I	365.0 366.3	.0019	.0032	.0007	.0018	$^3d_3$-$^3P_2$	1.3
Cd I	291.5	.0287	.0378	.0084	.0119		
Ni I	349.3 361.9	.1967	.201	.0753	.0833	$^3p_1$-$^3D_2$ $^1F_3$-$^1D_2$	1.02 0.66
Pb I	368.3	.2387	.2676	.2113	.259	$^2S_{1/2}$-$^2P_{3/2}$	1.5

GS # 1: Gallbladder Stone # 1, GS # 2: Gallbladder Stone # 2

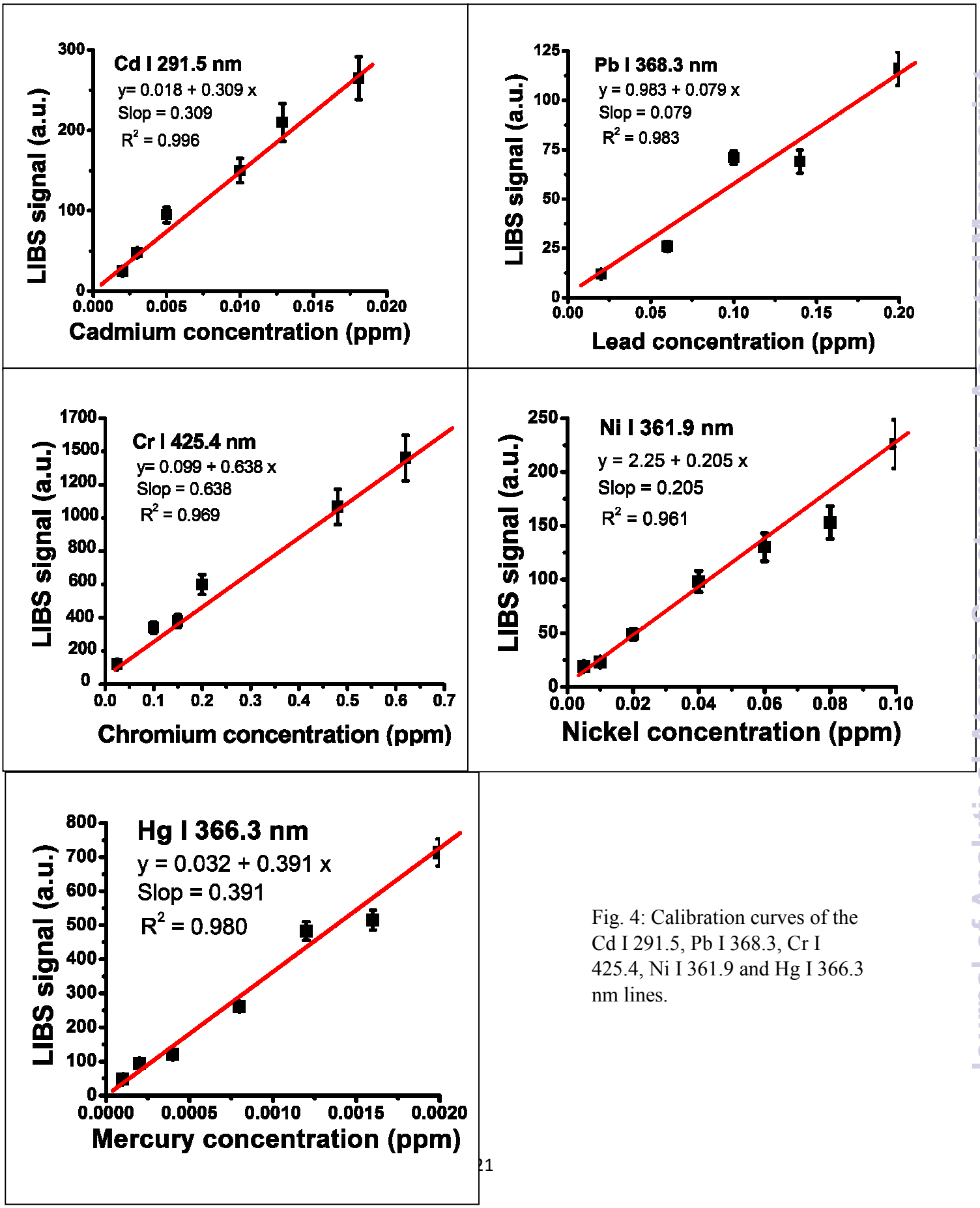

Fig. 4: Calibration curves of the Cd I 291.5, Pb I 368.3, Cr I 425.4, Ni I 361.9 and Hg I 366.3 nm lines.

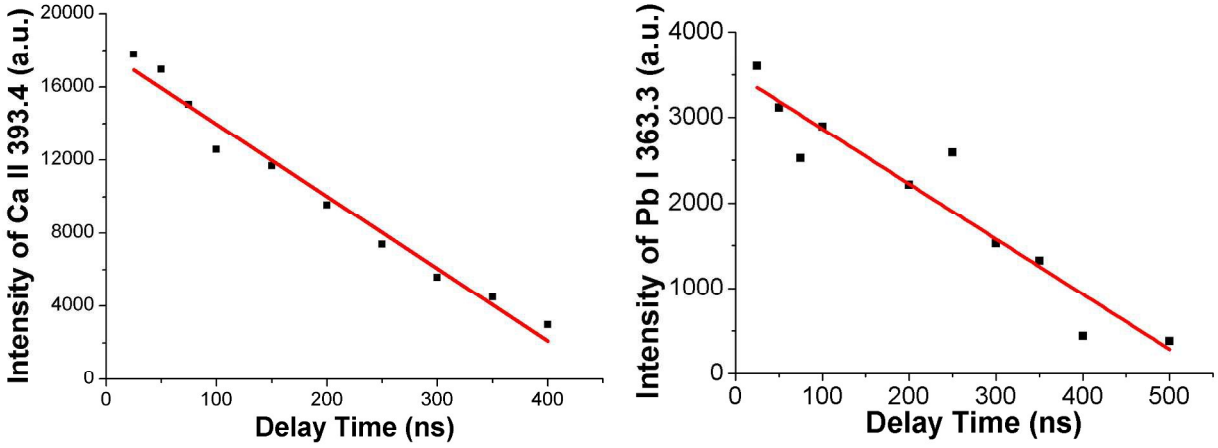

Fig. 5: Effect of delay time on the Ca II 393.4 and Pb I 363.3 nm lines.

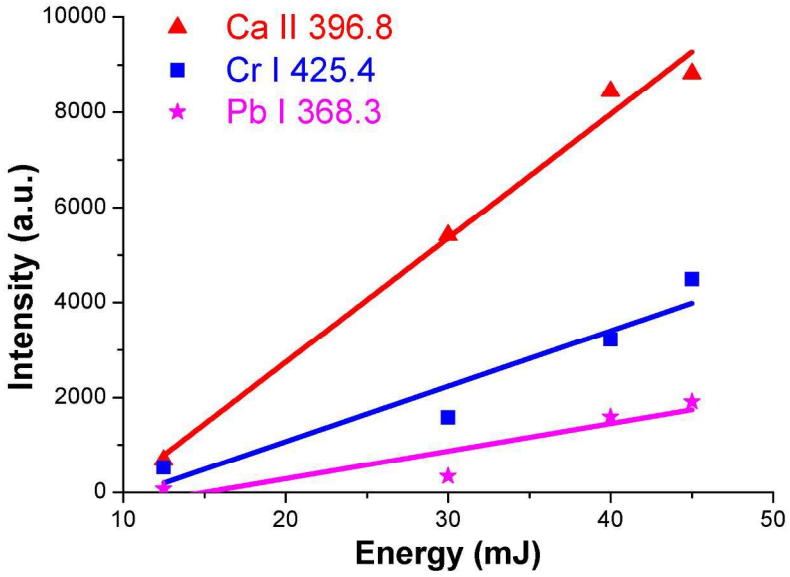

Fig. 6: Effect of laser energy on the Ca II 393.4, Cr I 425.4 and Pb I 368.3 nm lines.

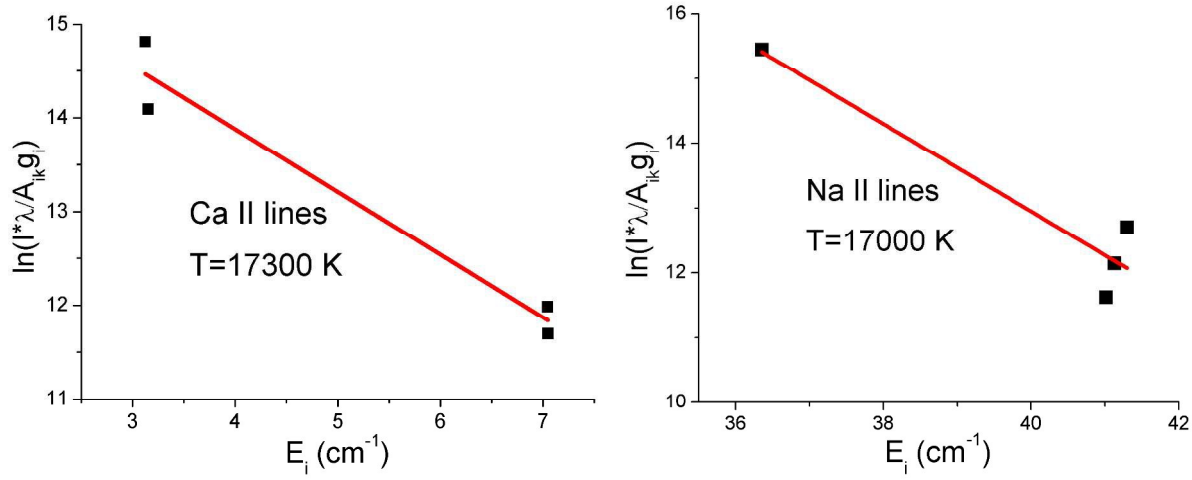

Fig. 7: Spectral lines intensity versus the energy of the higher states of the singly ionized calcium and sodium lines for plasma temperature calculation.

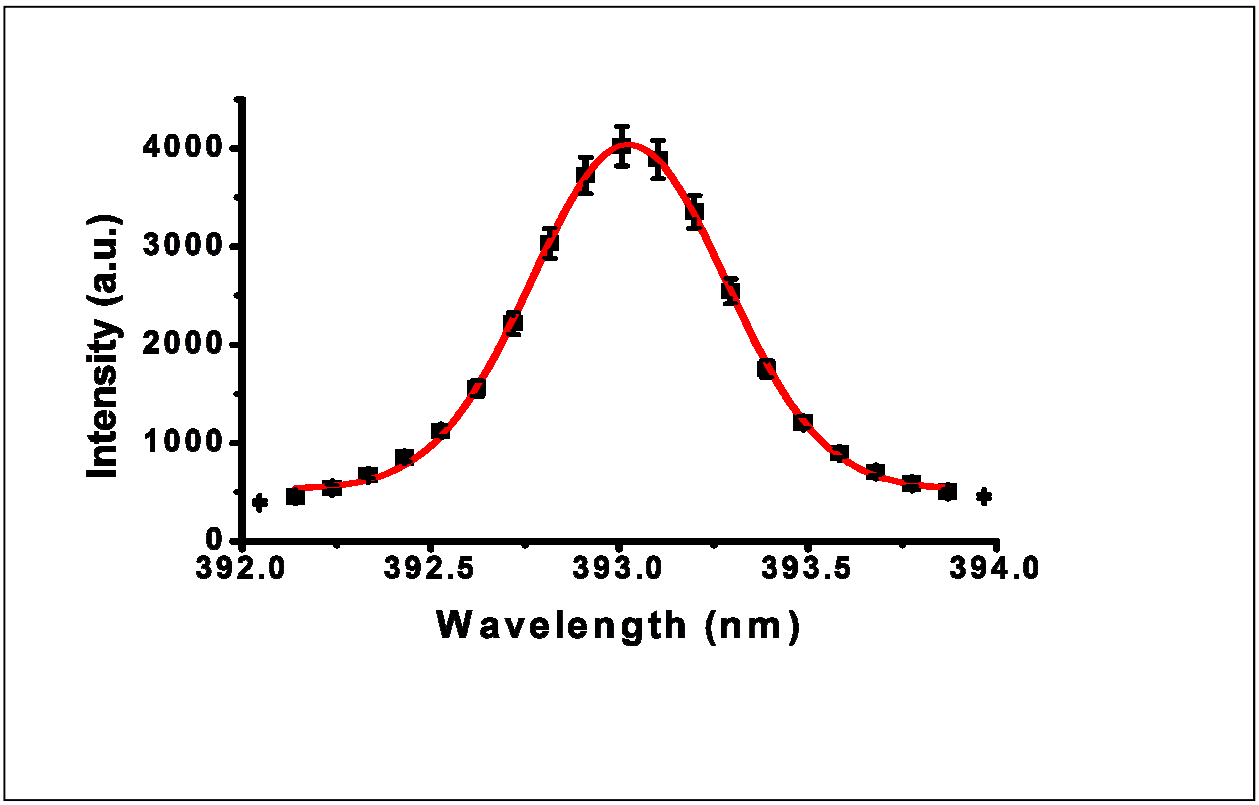

Fig. 8: Gaussian fitting of Ca II 393.4 line.

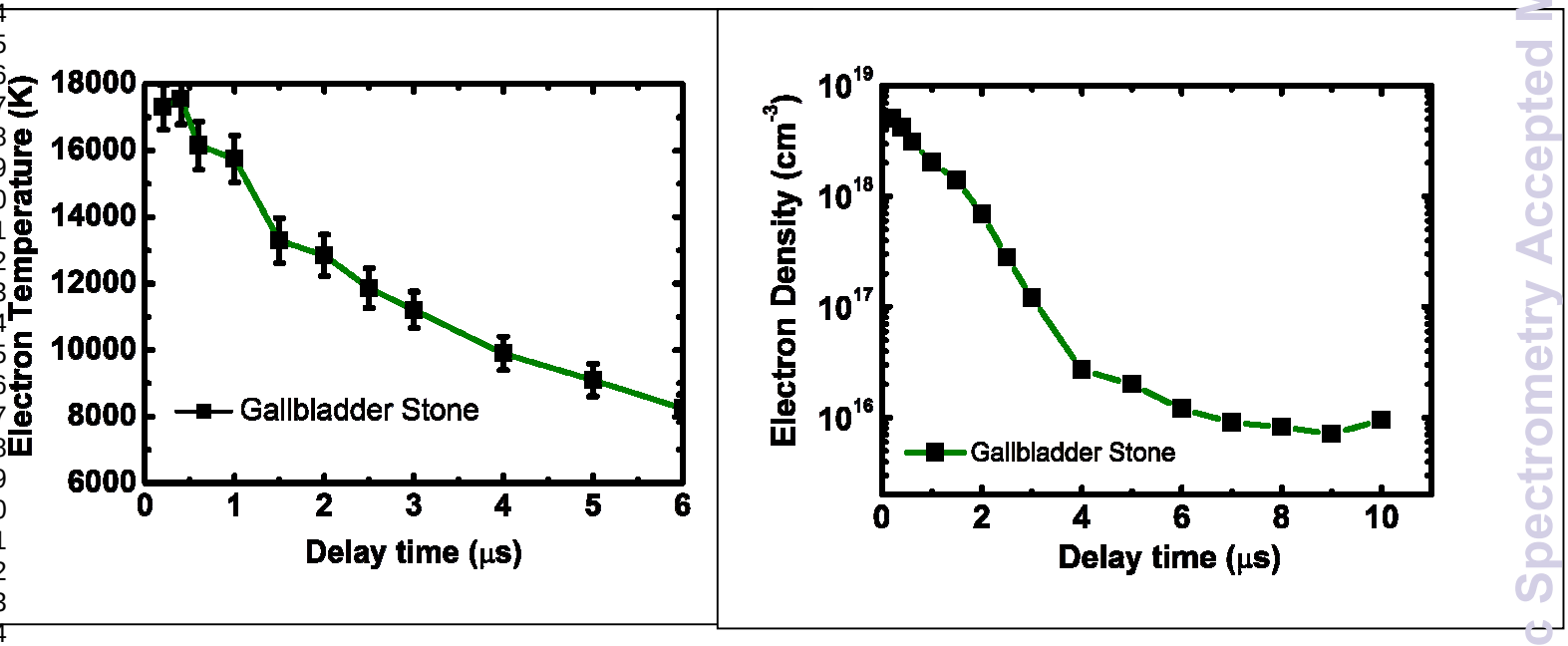

Fig. 9. Electron temperature (left) and electron density (right) measured at different delay times.

Laser Produced Plasma Diagnosis of Carcinogenic Heavy Metals in Gallstones

Mohammad A. Gondal[a*], Mohamed A. Shemis[a], Ahmed A. I. Khalil[b], Mohamed M. Nasr[c], Bilal Gondal[d]

[a]Physics Department, King Fahd University of Petroleum & Minerals, Dhahran 31261, Saudi Arabia

[b]Physics Department, Faculty of Science for Girls, University of Dammam, Dammam 31113, Saudi Arabia

[c]Preparatory Health Department, Riyadh Colleges of Dentistry and Pharmacy, Riyadh 11343, Saudi Arabia

[d]Department of Gastroenterology, Hepatology and Nutrition, The University of Chicago Pritzker School of Medicine, Chicago, IL 60637, USA